Structural analysis of two King-post timber trusses. Non-destructive evaluation and load-carrying tests

Jorge M. Branco, Maurizio Piazza and Paulo J.S. Cruz

August 11, 2009

Abstract

The misunderstanding of the overall behaviour of traditional timber trusses can result in incorrect strengthening interventions or, frequently, on their replacement. Timber roof structures need a more concise knowledge of the real behaviour to determine internal loads and control the load transfer. For that, laboratory tests on scaled or full-scale specimens of members, connections and trusses are needed.

In this paper, an accurate geometric and mechanical evaluation of the timber elements of two King-post timber trusses, based on grading results with data gathered from non-destructive tests (NDT), including mechanical evaluation of the modulus of elasticity in bending (MoE), followed by full-scale carrying tests were performed. The trusses were reassembled in laboratory and submitted to a series of symmetric and non-symmetric cyclic tests, according to the Limit States. Strengthening techniques evaluated in precedent research steps were used in a second phase of the load-carrying tests.

1 Traditional timber trusses

Trusses represent the most traditional timber structures with an extraordinary importance in the construction progress. The use of these structures is as old as mankind. In fact, the first timber trusses were used by primitive men as protection against the atmospheric agents, and since then, its presence in Architecture has been permanent. Although the low robustness of those structures lead to the survival of few examples, there are proofs that in Ancient Greece (4^{th} century BC) a well defined technique of construction of inclined timber roofs existed. The range of possible configurations in which it is practical to assemble different timber elements to form a truss is vast. Obviously, the selection depends on many factors: span, loads, roof inclination, etc. Nevertheless, the disposition of the different timber elements normally follow the rule that the shorter elements should work in compression and the longer in tension, thus preventing problems with buckling. In a plane structure, such as traditional timber trusses, submitted to concentrated loads on the joints, without bending of the members, stress distribution in the structure directly results from its geometry. However, this behaviour can be easily modified if the static model is changed. Assessment of constructed timber trusses shows various differences in their structural model. In fact, despite construction recommendations, intuitively developed over centuries by carpenters, it is common to find examples where they were not taken into account. Nowadays, the design of traditional timber trusses is a common topic in timber structures manuals (*e.g.*, Alvarez et al. (1996) and Piazza et al. (2005)). Usually, attention is focused on the overall static behaviour of trusses and the joints design. The truss timber elements are designed following the Eurocode 5 (2004) and some verification rules for the connections, derived from the possible failure modes, are given, since traditional carpentry joints are not directly analyzed in Eurocode 5. In the definition of the static model, loads

are assumed as point loads applied in the nodes and the joints are modelled as perfect hinges, despite their semi-rigid behaviour even when not strengthened (Parisi and Piazza, 2000). Timber roof structures require a more concise knowledge of the real behaviour in order to determine internal loads and control the load transfer. For seismic loading for instance, semi-rigidity and ductility are crucial for structural safety and analysis. The refurbishment of large historical roof structures requires the correct load transfer that can only be determined by means of an analysis when the real behaviour of wood material and connections is known.

2 Inspection and non-destructive evaluation

Visual inspections are the basis of any analysis of traditional timber structures. They enable detection of external wood decay, as well as of visible mechanical damages. Moreover, inspections can be used to characterize past or current dangerous climate condition, as evidenced by moisture stains on exposed surfaces. In current practice, visual inspection is coupled with non-destructive tests (NDT) (Piazza and Del Senno, 2001) in order to provide information pertaining to the properties, performance, or condition of the material and the structure.

Visual inspection is also a prerequisite to *in-situ* visual strength grading. Visual grading is based on the premise that mechanical properties of lumber differ from mechanical properties of clear wood due to several growth characteristics, which can be identified and evaluated visually. Visual strength grading procedures use empirical relationships, based on laboratory mechanical tests and statistical relationships, to assign lumber members to an established strength class by measuring some visual features, such as growth characteristics, surface decay and geometrical features.

NDT can be classified in two distinct groups: global test methods (GTM)

and local test methods (LTM) (Bertolini et al. (1998) Ceraldi et al. (2001)). The former includes, among others, the application of ultrasonic and vibration methods. The latter includes the Resistograph® (Rinn, 1992) and the Pilodyn® (Görlacher, 1987), which usually plays a major role in the support of visual inspection of wooden elements and, consequently, structures. GTM represent techniques difficult to implement *in-situ*, more appropriate to laboratory facilities. Their advantage is the global evaluation of the material that they allow, overlapping small local defects which could reduce the mechanical evaluation of the entire piece. Usual applications of LTM are related to the prediction of the element residual section by analyzing abnormal density variations in the element generally associated with mass loss, resulting from biological degradation (Machado and Cruz, 1997). If some precautions are not taken into account, LTM may represent only the evaluation of a small part of the material. This kind of techniques requires a considerable number of test results to be representing of the entire piece. Fortunately, usually, those non-destructive tests are easy to handle.

3 Trusses evaluated

The two full-scale timber trusses studied in this work were recovered from a construction located in Caldonazzo Lake, Italy. The date of the construction is not well known but it is supposed that the timber trusses are more than seventy years old. Still in place, the trusses were marked and every member was named to enable the dismantling and transportation phases in safety, preventing eventual errors in the assembling process in laboratory. The trusses were stored for four years in the Materials and Structural Testing Laboratory of the University of Trento, Italy. Figure 1 shows the geometry of the trusses evaluated and the rule adopted for the numbering of the elements.

4 Non-destructive evaluation of the trusses

Using test methods from both NDT groups, GLM and LTM, trusses were submitted to an accurate geometric and mechanical evaluation. After a detailed visual inspection, timber elements were visually graded. The geometric properties were recorded and references cross sections were defined. Pilodyn®, Resistograph®, hardness test, as LTM, Sylvatest® and the mechanical evaluation of the modulus of elasticity in bending (MoE), as GTM, were used to evaluate the biological and mechanical condition of the timber elements. The moisture content was measured and the density of each timber element was quantified.

4.1 Geometric assessment

All truss elements consist of one single timber piece causing significant variability in the cross-section area of the elements observed, in particular in those longer, like the tie beams. In order to have an adequate report of all those variabilities of the truss geometry, a geometric assessment was performed. Every 40 cm, each element was marked, named and the cross section measured. Those cross-sections were used also in the non-destructive tests conducted and reported in following items. Figure 2 presents the cross section A of the tie beam of the *Truss* 1, as example of the difference that can be obtained if an inadequate measurement of the cross-section is performed.

4.2 Moisture content

The moisture content determination for each timber element was based on three readings using a thermo hygrograph following the measuring scheme of UNI 11035-1 (2003). No significant variations between all moisture content values were detected, Table 1. All members of *Truss* 1 present an average value of

the moisture content between 11.3% and 12.5% while for *Truss* 2, all members present an average value for the moisture content in the range 12.1% - 12.7%.

4.3 Density evaluation

The density of wood is, on one hand, an extremely variable property, but on the other, a very important one since the mechanical performance of wood is closely related to it. The density of wood is a measure of the amount of cell-wall material relative to the size of the cell cavities. Consequently, density is connected first with the relative proportions of the different types of cells present, and second to the absolute wall thickness of any one type of cell. Density is certainly one of the two most important parameters determining the mechanical performance of wood (Dinwoodie, 1989).

The volume obtained from the geometric assessment was considered equal to the apparent volume of wood (V_{app}) because as no significant cavities caused by deterioration or/and shrinkage were detected, the process used to measure the volume was significantly accurate, and the moisture content present by all elements is very near to the reference value (12%). For the wood species evaluated, *Picea abies* Karst., a density value of 415 kg/m^3 was expected, according to UNI 11035-2 (2003), value not far from the range values measured for timber truss elements (384 kg/m^3 - 479 kg/m^3), see Table 2.

4.4 Visual grading

The grading criteria according to the European EN 518 (1997) and the Italian national standards UNI 11035-1 (2003) and UNI 11035-2 (2003) have been applied. UNI 11035-1 (2003) defines terminology and measurement of features for the visual strength grading of Italian structural timbers. Hence, it defines reference moisture content, direct or indirect evaluation of the density, the latter

performed by measuring the number of growth rings contained in a reference line, limits to defects reducing the strength (knots, slope of grain, checks, splits, shakes), limits to geometrical features representing growth defects (wane and warp) and decay. The second part of the code, UNI 11035-2 (2003), contains visual strength grading rules and characteristic values for Italian structural timber population. Grading rules are specified for different Italian timbers that are identified by coupling species and provenance. Timbers are assigned to strength classes by measuring the visual features specified in the first part of the code. Finally, strength values are assigned to strength classes for each timber group.

The species of the two King-post trusses analysed is Spruce (*Picea abies* Karst.), from North Italy. Accordingly, grading criteria referred to the group 'softwood 1' in UNI 11035-1 (2003) § 5.3 have been adopted. Unlike an on-site inspection, it was possible to examine, in laboratory, all the faces and ends of the elements. Each element face and each face portion (approximately 40 cm wide) has been numbered by means of a section. Hence, all the defects present on each face, were localized, measured and mapped.

According to UNI 11035 (2003), single knots were measured considering the ratio A of the minimal diameter to the width of the element face, while knot clusters were evaluated through the ratio A_g of the sum of the minimal diameters of all the knots, in a 150 mm range, to the width of the element face. General slope of grain was detected by means of a scribe, or when present, by measuring shrinkage splits on the longitudinal faces. Table 3 presents the visual grading results for both trusses timber elements.

4.5 Non-destructive tests

4.5.1 Hardness test

Hardness is generally defined as resistance to indentation. Actually, wood hardness involves compression, shear strength and fracture toughness. Wood hardness is positively correlated to density, and as a consequence to the material strength properties. Moreover, hardness is in inverse proportion to the moisture content. In the performed tests, according to Turrini and Piazza (1983), hardness has been estimated by measuring the load force R required to embed 5 mm a 10 mm diameter steel hemispherical bit, where the test area must be clear, that is, without visible defects, Figure 3. The value of R was obtained by averaging the test results made in the four longitudinal faces of the element, in numbered sections every 80 cm wide. Each test consisted of five measures taken in each tested area. The result of each test was obtained by averaging the three middle values among the five measures. It means that, for each considered section 20 tests were carried out (four per surface): 9 for the tie beams, 5 for the rafters and 2 for the struts and king posts, making a total of 1000 hardness tests performed.

The correlation between R and the module of elasticity in bending (MoE) is expressed by the experimental equation:

$$MoE = \delta \cdot 350 \cdot R^2 \tag{1}$$

where δ indicates a reduction factor, $0.5 \leq \delta \leq 0.8$, that depends on the defectiveness of the element.

Because the Equation 1 is experimentally founded, its reliability depends on the limits of the experimentation itself, namely on the species of the tested samples that are Silver fir (*Abies alba*) and Larch (*Larix decidua*), on load force

R (700 ÷ 3000 N) and moisture content in the range of 12% - 14%. Due to the large amount of hardness tests performed and since mechanical determination of the elastic modulus of some elements (tie beams and rafters) is available, it was possible to calibrate the equation for the case of Spruce (*Picea abies* Karst.). Based on the experimental results for the modulus of elasticity in bending (MoE), the δ factor was accurately calibrated. For the truss members in which the MoE was mechanically assessed, a range between 0.58 and 0.65 was found for the calibrated δ factor, see table 5.

The local nature of the hardness test requires a local evaluation of the defectiveness factor δ. The visual grading is based on the evaluation of local defects but the result is the assignment of the entire timber element to a specific strength class. Therefore, the local assessment, or in other words, the evaluation of the local defectiveness, is not directly measured through the visual grading. Otherwise, based on the correlation between the visual grading and the evaluation of the defectiveness, the definition the δ factor could be possible in the case of the members not mechanically evaluated (MoE). In order to exceed this difficulty, and because the δ factor calibrated presents a minor variation (Coefficient of Variance equal to 5.24%), the adjustment of a single δ value for all timber elements ($\delta = 0.6$) was performed. The elasticity modulus of each element, estimated by means of the hardness test, is reported in Table 4.

4.5.2 Pilodyn®

The Pilodyn® method uses a steel pin of a fixed diameter driven into the material by a dynamic force. The depth of penetration is correlated with material density. Görlacher (1987) developed relationships between the depth of penetration of a standard pin and the density of the wood. The correlation coefficient varied from 0.74 to 0.92, depending on the number of measurements and species. The empirical relationships are obviously affected by moisture content. For all

elements that compose both trusses, in each section used for the geometric assessment, the penetration depth obtained through the Pilodyn® in the 4 faces was measured, in a total of 548 tests. Table 6, presents the average values of the depth penetration measured for each element of both trusses. A linear correlation between density and depth penetration seems adequate to represent the test results, despite the lower coefficient of determination $R^2 = 0.50$ (Figure 4).

4.5.3 Resistograph®

The use of a small-diameter needle-like drill was introduced by Rinn (1992). The cutting resistance of a needle is recorded as a function of depth as the needle penetrates the timber. The resulting profile can be used to determine the location and extent of voids and variation in material density. This technique is highly effective for quantifying the extent of deterioration in timber.

Some researchers have tried to use the results of the resistograph® as prediction of the mechanical properties. For example, Feio (2005) compared the resistance drilling achieved with resistograph® directly with destructive tests. For that, he used the Resistance Measure (RM), given by the quotient between the integral of the area of the resistograph® chart and the depth penetration of the nail in the specimen, equation 2.

$$RM = \frac{\int_0^{depth} Area}{depth} \tag{2}$$

Feio (2005) showed that the correlation between the RM value and measured density is $R^2 = 0.71$ for new timber and $R^2 = 0.68$ for old timber. RM had a correlation to modulus of elasticity of $R^2 = 0.60$ for new timber, and $R^2 = 0.64$ for old timber. Correlation of RM to longitudinal compressive strength was

shown to be $R^2 = 0.59$ and $R^2 = 0.64$ for new and old timber respectively.

However, the use of the RM value to estimate mechanical properties is questionable (Lear, 2005). The area of a resistance-drilling plot can be affected by multiple parameters including drill bit sharpness and general equipment use such as drill orientation. On a single member, changes in the orientation of the drill with respect to growth rings will change the calculated RM value with each drilling. Nevertheless, resistance drilling can be used to estimate mechanical properties of members based on the quantification of deterioration and basing calculations on the remaining sound material and information on clear strength that can be estimated with other non- and semi-destructive testing.

In this work, resistograph® was used mainly with the purpose of detecting deterioration and evaluating the voids existing inside the timber members. The main objective of using this technique was not to predict mechanical properties but to complete the information given by the other non-destructive tests realized. In particular, the evaluation of the deterioration level and the voids existing inside the members, and for that, not visible, were the main purpose of the use of resistograph®. In each element of the two trusses, a small number of sections was selected, in which two resistograph® charts were collected (one in direction perpendicular to the other). Forty one and thirty six tests were performed in *Trusses* 1 and 2, respectively, however, no sustainable correlation between the RM and density was found.

4.5.4 Sylvatest®

The ultrasound device Silvatest® allows sending and receiving a longitudinal ultrasound wave using two piezoelectric probes. It measures the duration of the stress wave course in the tested sample, with regard to its moisture content and temperature, which are also controlled. Since there is a one-to-one relation between this speed and the mechanical and physical properties of timber (elasticity

modulus and density), the instrument directly displays the measured mechanical quality after taking the influence of humidity and temperature of the timber into consideration. In order to assess the influence of the test method on the results, both methods were applied whenever possible. Each single measured value represents the third reading value, to avoid bigger variability in the test results. As pointed out above, after the entry of the distance between the two ultrasonic sensors ($Length$), the Sylvatest® instrument shows the time spent by the ultrasonic wave ($Time$), the measured mechanical quality is displayed ($Class$) and mechanical values for the elastic modulus in bending (E_{b}) and the allowable bending strength (F_{b}) are proposed. As an example, in Table 7, the test results of the Sylvatest® for one rafter of the *Truss* 2 (Rafter 22), considering both measurement methods, are reported. Different measurement methods and probe position led to different Sylvatest® results. Using the indirect method in two different longitudinal faces, between the same sections, inconsistency in the results is again obtained. This discrepancy is more evident in the allowable bending strength (F_{b}), less important for the elastic modulus in bending (E_{b}) and disappears for the measured mechanical quality class. In consequence, it was decided that, whenever the results of the Sylvatest® are compared with others results achieved by the non-destructive evaluation performed, the values obtained using the direct method are assumed. By the way, the speed of ultrasound waves is "physically" directly correlated only with material density and material modulus of elasticity. Table 8 shows the Sylvatest® results obtained using the direct method, when possible, for all elements that composed the two trusses.

4.5.5 Mechanical evaluation of the modulus of elasticity in bending

The stiffness of the timber elements of both trusses, which is normally expressed as MoE (Modulus of Elasticity in bending), was determined by means of bend-

ing tests. MoE for timber contains not only information about the clear wood strength properties, but also to a large extent about defects affecting the stiffness. Therefore, results of bending tests have been used in this research to assess the reliability of visual grading and NDT results. Static bending tests were conducted in accordance with the four-point loading method, with reference to EN 408 (2003). Because of the large span needed for the correct execution of the bending tests (18 times the depth), only the rafters and the tie beams were tested. Results of the four-point bending tests are reported in Table 9.

4.6 Analysis and discussion of NDE

During the visual inspection, significant variation in cross-section geometric properties was found. Indeed, as all elements of the trusses are composed of one single timber piece, important deviations are expected, as consequences of the changes in the cross-section of the trunk. Using UNI 11035-1 (2003) and UNI 11035-2 (2003) it was possible to visually grade the strength of the timber elements. In particular, a strength class was assigned and an average value for the modulus of elasticity (MoE) was suggested. Three values for MoE were found: 12000 MPa, 10500 MPa and 9500 MPa corresponding to the three strength classes considered in those standards, S1, S2 and S3, respectively. For visual grading, there was the necessity of recording the moisture content and calculating density. No significant variations between moisture content values were detected. All members of $Truss$ 1 present an average value for the moisture content between 11.3% and 12.5% while for $Truss$ 2, all members present an average value for the moisture content in the range 12.1% - 12.7%. A density range of 384 kg/m^3 to 479 kg/m^3 was obtained for the timber truss elements in accordance with the reference value suggested by UNI 11035-2 (2003) for *Picea abies* Karst. (415 kg/m^3). The hardness test developed by Turrini and Piazza

(1983) permits the correlation between the load force (R) required to embed a steel bit into the wood with MoE. However, a reduction factor depending on the defectiveness of the element is needed. This reduction factor was calibrated (a value of 0.6 was found) using 760 hardness tests results and the MoE values obtained with the mechanical evaluation of the tie beams and the rafters of both trusses. Despite the considerable quantity of values used, the correlation found between the load force (R) and the density (ρ) is poor ($R^2 = 0.35$). Others researchers, Feio (2005) and Lear (2005), have tried to correlate the Resistance Measure (RM), obtained with the Resistograph® test, with density. The same attempt was made but the correlation obtained was very poor ($R^2 = 0.02$). The difficulties involved in this kind of test have already been pointed out. The area of a resistance drilling plot can be affected by multiple parameters including drill bit sharpness and general equipment use such as drill orientation. These uncertainties are amplified in the case of old timber elements, with splits and slope of grain caused by moisture content variation and shrinkage. These defects have a significant impact in the area of the resistance drilling plot used to calculate RM. As conclusion, and assuming the mechanical evaluation of the MoE as reference, correlation between the results of the non-destructive tests and MoE obtained through mechanical evaluation are low, as shown in Figure 5. A very poor correlation ($R^2 = 0.06$) was established between the MoE given by the visual grading and the one resulting from the mechanical evaluation. A correlation presenting $R^2 = 0.15$ was defined between the Sylvatest® results for the MoE and the values found through the mechanical evaluation. An interesting correlation, $R^2 = 0.62$, was obtained between the Turrini-Piazza hardness test and the mechanical evaluation, in terms of MoE prediction. Sandoz et al. (2000) state that non-destructive testing by means of ultrasound overestimates mechanical properties in 25%. Moreover, old wood generally presents higher

mechanical properties in comparison with recent plantation growth trees. Difference between old and new wood properties results in diverse velocity due to different wood density (Ehlbeck and Gorlacher, 1990). Görlacher (1991) investigated the correlation between modulus of elasticity and strength of old wood and considered that correlation coefficients are approximately the same for old and new wood. However, Kasal and Anthony (2004) found only a weak correlation between ultrasound pulse velocity methods and ancient wood member density.

5 Load-carrying tests

Trusses were subjected to cyclic tests, under symmetric and non-symmetric loading for two levels of loads corresponding to the Serviceability and Ultimate Limit States. Considering their behaviour under this series of tests, the trusses were strengthened. Later, the same sequence of tests was carried out over the strengthened trusses. If, after that, the failure of the truss had not been achieved, a final test under growing loading was performed. In the following, the main conclusions of the tests results are presented.

5.1 Test setup, instrumentation and procedure

The timber trusses were tested under cyclic loading subjected to two point loads, each one directly applied over the strut-rafter joint. Symmetric and non-symmetric tests were performed using two load values, corresponding to Service and Ultimate Limit States (SLS and ULS, respectively). The loads considered include self-weight of the original timber roof and the snow load corresponding to the location of the trusses, Caldonazzo Lake (500 m of altitude). Before the load-carrying tests, and after the reconstruction of the disassembled trusses, trusses were subjected to a series of loading and unloading tests aiming at ad-

justing all truss elements together reducing to the minimum the free movements between them. The first step of the load-carrying tests was the application of the load corresponding to the self-weight of the timber roof (covering material and structure and purlins). After that, the remaining load corresponding to each loading case was divided into four steps. Therefore, the load target was reached after 4 cycles of loading and unloading keeping constant the minimum load applied corresponding to the self-weight. In each test carried out, three cycles were performed (Figure 6). The non-symmetric test results from the asymmetric value of the snow load should be considered in accordance with D.M. 14/9 (2005).

During the tests the main global displacement of the trusses, the relative displacement between the king post and the tie beam and the rotation of each joint were measured, using for that fourteen transducers. Two manual hydraulic jacks, supported by a steel frame fixed to the reaction slab of the laboratory, were used for applying the loads. Moreover, those two frames were used to laterally restrain the trusses. Two supports restraining the vertical displacement were placed at each end of the truss, having the right support the horizontal movement also restrained. Figure 7 shows a general overview of the test setup and measurement layout used in the tests and Table 10 summarizes the load-carrying tests performed on both trusses.

In terms of the test designation, the first letter can be an S or a U corresponding to the Service or Ultimate Limit States, respectively, the second letter is a U or an S in the case of unstrengthened or strengthened conditions, respectively, and in the third position, there is an S for the case of symmetric test, Dx when the maximum point load is F_{Dx} and Sx if F_{Sx} is the higher point load. The test "Failure" corresponds to the one performed to obtain the failure of the truss.

5.2 Evaluation of the trusses behaviour

The response of both trusses under the different tests performed is highly dependent on the variability, previously detected and reported, along the truss members in terms of cross sections area and principal moments. Moreover, the difficulty associated with tests over existing structures is recognized, in which the members can present residual deformations and signs of degradation and/or the connections are not well tight. The tests results show that even under symmetric loading conditions, the behaviour of both trusses is non-symmetric. This conclusion is more evident in the response of $Truss$ 1 under symmetric loading corresponding to SLS (Figure 8).

The connection between the king post and the tie beam, made by a steel rod of 20 mm diameter fixed in the king post, aligned in its longitudinal direction, passing through the tie beam and having one nut in the extremity, fastening the two elements, performs adequately. An increase of the relative displacement between those two elements is avoided and a negative displacement (king post approaching) is allowed (Figure 9).

As consequences of the trusses deformations under the vertical loads applied, horizontal displacements of the non-restrained support in the horizontal direction were recorded (Figure 10).

Under non-symmetric loading conditions, the asymmetric behaviour of the trusses, already pointed out, is emphasised. Channels A6 and A7 show non-symmetric displacement and the horizontal movement in the bottom of the king post, recorded by channel M1, is largely higher than under symmetric loading, Figure 11. This asymmetric behaviour of the trusses introduces bending stress in the rafters and tie beam. Due to the rotational stiffness of the king post-tie beam connection, the asymmetric response of the overall truss induces distortion in the tie beam (Figure 12). This distortion induces important bending stresses

in the bolt of this connection (Figure 13).

The connection between the king post and the tie beam presents rotational stiffness in both the plane of the truss and the perpendicular one to it. Therefore, this connection also prevents the out-of-plane movement consequently improving the stability of the substructure composed by the rafters, the king post and the struts (Figure 13).

As expected, under non-symmetric loading, the relative displacement between the king post and the tie beam, measured in the connection between both elements, is nearly zero. In addition, the horizontal movement recorded in the non-restrain supports is reduced. In the case of the Ultimate Limit State (ULS), different behaviour was observed for both tested trusses. While $Truss$ 2, was able to sustain all tests (symmetric and both non-symmetric), in $Truss$ 1 only the first cycle of the symmetric tests was finished. When the maximum load corresponding to this limit state was reached, considerable out-of-plane movements were visible (Figure 14). To prevent the global failure of the truss, the test procedure was stopped and $Truss$ 1 was strengthened before proceeding with the experimental program.

In the case of $Truss$ 2, the tests undertaken for SLS were repeated for the load level corresponding to the ULS. The main conclusion about the overall behaviour of the truss pointed out for the SLS can be extended to ULS. Therefore, one may conclude that, apart from the instability observed in the case of $Truss$ 1, the truss safety under ULS was verified. No local collapse or failure in the timber members occurred. It is important to point out that the bracing forces transmitted by the purlins and the covering structure, boundary conditions existing on-site, should be able to prevent the instability observed in the case of $Truss$ 1 load-carrying tests.

5.3 Strengthening

In the next load-carrying test phase, trusses were strengthened based on the response obtained in first tests, and the strengthening effectiveness was assessed through the same test history. Strengthening aimed at improving the overall behaviour of each truss, preventing local failures that could hamper the complete test history defined.

Strengthening of *Truss* 1 aimed essentially at repairing the out-of-plane movement observed and preventing this instability, allowing tests corresponding to the ULS. The out-of-plane deformations were removed and a UPN profile was bolted to the king post. The objective was to prevent the out-of-plane movements, increasing the stiffness of the connection in this direction, keeping the tie beam suspended to the king post (Figure 15a). The timber elements did not presented any local failure or damage. However, the connections between the rafters and the tie-beam were weakened, particularly the left connection, over the support with horizontal displacement. The depth of the step was insufficient and the timber in the notch front showed some fissures. Therefore, this part of the tie beam (beyond the step) was strengthened with screws (12 screws M6-200) in order to increase its shear resistance. Moreover, using the pre-existing holes, an internal bolt of 20 mm diameter was introduced at mid joint, normal to the rafter in each rafter-tie beam connection (Figure 15b). Similar bolts existed in those connections before the dismantling of the trusses.

In the case of *Truss* 2, only the connections between the rafters and the tie beam were strengthened. The stiffness of the king post-tie beam connection proved adequate to prevent the instability of the truss. Rather, the timber beyond the step displayed some signs of deterioration and the depth of the steps in the rafters/tie beam connections appeared insufficient. The same strengthening technique used in *Truss* 1 was applied: one internal bolt tightening the con-

nection and screws beyond the step to improve the shear resistance. However, and as an improvement based on the failure modes observed in *Truss* 1 tests, a binding strip was used to confine the timber in the front notch (Figure 16).

5.4 Efficiency evaluation of the strengthening

The series of tests corresponding to the SLS were repeated after the truss strengthening. The objective was to analyze the influence of the stiffness of the tie beam-rafter connections, in the overall behaviour of the truss, in particular, under non-symmetric loads. Nevertheless, the main goal of the strengthening was to increase the truss load capacity: to make *Truss* 1 able to perform all load procedures corresponding to ULS and to assess the failure load of *Truss* 2.

The load capacity of *Truss* 1 was improved by the strengthening but only the symmetric test corresponding to the ULS was accomplished. At the end of this test, the local damages in the tie beam-rafter connections hampered the execution of the non-symmetric tests. In consequence, the decision was to proceed with a symmetric load test until failure. It is important to point out that the ultimate load achieved in the failure test was lower than the load level attained in the precedent ULS test. Despite the strengthening measures undertaken to improve it, the failure was caused by lack of shear resistance of the tie beam in the notch front. Theoretically, the presence of the screws should have increase the shear resistance but, because of the fissures already existing before placing the screws, the timber part in the notch front did not work as a rigid body. The screws expanded the fissures and the rigid body split in small pieces (Figure 17a). Moreover, the failure of this connection was caused by a previous shear failure of the rear step (Figure 17b). With the horizontal movement of the rafter in the connection tie beam-rafter, the joint king post-struts was dismantled (Figure 17c) and important bending stresses

were introduced in the internal bolt (Figure 17d).

In the case of *Truss* 2, it is difficult to conclude if the strengthening was efficient in the improvement of the truss load capacity, as no failure was obtained in the tests performed in unstrengthened conditions. The strengthened truss was subjected to the entire test history (SLS and ULS, under symmetric and non-symmetric loads). After that, a load procedure until failure followed. This procedure was similar to the previous but now, the load increment did not stop at the value of 80 kN (maximum point load corresponding to ULS). The maximum point load value achieved in the failure tests was 100 kN. Again, the failure of the truss was obtained by shear failure in the timber in front of the notch in the connection tie beam-rafter. First, the shear failure of the rear step happened and then the shear failure of the timber in the front part of the notch took place (Figure 18).

Failure was defined by the geometry of the tie beam-rafter connections (Figure 19) and happened in the double step connection in which the rear step presented a bad geometry (connection in the right side). The rear step must be deeper than the frontal one. If not, the surface resisting to shear stress is insufficient. The double step connections of the right side (over the fixed supports) failed as a consequence of a first shear failure in the rear step. Once the rear step failed, the stresses concentrated in the frontal step. As the frontal step geometry was not enough for the stresses level applied, the complete failure of the joint took place.

5.5 Strengthening influence

Strengthening aimed at correcting local failures and improving the trusses load-capacity. Nevertheless, strengthening had influence in the overall behaviour of the trusses during the test history performed. A detailed analysis of the test

results obtained in terms of joints rotations and displacements measured in the most relevant points during the tests performed (Table 11 in the case of *Truss* 2) shows that:

- Strengthening reduced the distortion of the trusses, observed even under symmetric loading and measured by the horizontal movement of the bottom of the king post (LVDT called M1);
- Strengthening was able to reduce the deformation of the trusses by increasing the axial stiffness of the rafter-tie beam connections and by allowing the moment-rotation behaviour of these joints minimising pinching;
- Strengthening reduced the joints rotations, not by a significant increase in the stiffness value but, essentially, reducing the pinching effect observed in the unstrengthened conditions. In particular, in the first load cycle, the connections of the unstrengthened trusses presented significant pinching (Figure 20);
- In some cases, unstrengthened connections shows nonlinear behaviour with an elasto-plastic phase in the moment-rotation (M-R) curves. On the contrary, strengthened connections exhibited a full elastic M-R behaviour;
- In $Truss$ 1, the strengthening of the left tie beam-rafter connection became efficient only during the 2nd and 3rd load cycle as a result of the gap existing in the pre-existing hole used to insert the bolt. The opposite connection, strengthened with the same technique but using a new hole, was efficient since the beginning of the tests;
- In $Truss$ 2, rotation measured in the left tie beam-rafter connections was always higher than the ones registered in the similar connections located in the opposite side of the truss. Note that the right connection failed in

the ultimate tests. The rotation capacity of this connection was reduced in consequence of the movement introduced by the shear failure in the front part of the notch which caused the failure of the truss;

- In $Truss$ 2, strengthening results in displacements variation, in comparison with the unstrengthened conditions, were not significant, mainly below 20% and with higher values in the SLS case, with the exception of the horizontal movement of the king post bottom (recorded by M1) which, in some load cases, presented a reduction of 73%;

- In the case of $Truss$ 2, under non-symmetric loading conditions and for the ULS load level, the effect of the strengthening in the vertical displacement recorded is very limited.

5.6 Conclusions

The load-carrying tests of both trusses were preceded by an extensive ND evaluation of the timber elements. Weak correlations between the ND tests performed and destructive tests were obtained. Even in laboratory conditions, when evaluating real-size old timber elements (and not using manufactured specimens) ND evaluation is a very hard task that should be based on a wider range of ND tests available. Low correlations between the results of the non-destructive tests and MoE obtained through mechanical evaluation were obtained. The more reliable correlation was obtained with the Turrini-Piazza Hardness tests. Therefore, more investigations are needed on the ability of using NDE to accurately assess the MoE of in-situ timber members. The detailed geometric assessment performed revealed to be of crucial importance, not only in the interpretation of the ND evaluation but especially regarding the analysis of the load-carrying test observations and results.

Load-carrying tests confirmed the need to strength connections. Strengthening improves the resistance of the trusses and, in particular, their overall behaviour under non-symmetric loading conditions. The connections between the tie beam and the rafters and the tie connection that suspend the tie beam to the king post are the most important. The first are the most loaded and the last is of particular importance when the truss is subjected to distortion, caused specially by non-symmetric loads. The geometry of the connections proved of significant influence in the behaviour of the connection and, consequently, in the truss behaviour.

References

Alvarez, R., Martitegui, F., and Calleja, J. (1996). *Estructuras de madera - Diseño y cálculo*. AITIM, Madrid, Spain.

Bertolini, C., Brunetti, M., Cavallaro, P., and Macchioni, N. (1998). A non-destructive diagnostic method on ancient timber structures: some practical application examples. In *Proceedings of the 5th World Conference on Timber Engineering*, volume 1, pages 456–465, Montreux, Switzerland.

Ceraldi, C., Mormone, V., and Ermolli, E. (2001). Resistographic inspection of ancient timber structures for the evaluation of mechanical characteristics. *Materials and Structures, RILEM*, 34:59–64.

Dinwoodie, J. (1989). *Wood: Nature's cellular polimeric fibre-composite*. The Institute of Materials, London, UK.

D.M. 14/9 (2005). *Norme tecniche per le costruzioni*. Decreto Ministeriale, del Ministero Infrastrutture e Transporti, published on official gazettente Nazionale Italiano di Unificazione.

Ehlbeck, J. and Gorlacher, R. (1990). Zur problematik bei der beurteilung der tragfahigkeit von altem konstruktionsholz. *Bauen mit Holz*, 2(90):117–120.

EN 408 (2003). *Timber structures. Structural timber and glued laminated timber. Determination of some physical and mechanical properties*. European Committee for Standardization.

EN 518 (1997). *Structural timber. Grading. Requirements for visual strength grading standards*. European Committee for Standardization.

Eurocode 5 (2004). *EN 1995-1-1: Design of timber structures - Part 1-1: General - Common rules and rules for buildings*. European Committee for Standardization.

Feio, A. (2005). *Inspection and Diagnosis of Historical Timber Structures: NDT Correlations and Structural Behaviour*. PhD thesis, University of Minho.

Görlacher, R. (1991). Untersuchung von altem konstruktionsholz: Bestimmung des elastizitatsmodulus. *Bauen mit Holz*, 8(91):582–586.

Görlacher, V. (1987). Zerstörungsfreie prüfung von holz: ein in situ verfahren zur bestimmung der rohdichte. *Holz als Roh- und Werkstoff*, 45(7):273–278.

Kasal, B. and Anthony, R. (2004). Advances in *in situ* evaluation of timber structures. *Progress in Structural Engineering and Materials*, 6(2):94–103.

Lear, G. (2005). Improving the assessment of in situ timber members with the use of non-destructive and semi-destructive testing techniques. Master's thesis, North Carolina State University.

Machado, J. and Cruz, H. (1997). Avaliação do estado de conservação de estruturas de madeira. Determinação do perfil densidade por métodos não destrutivos. *Revista Portuguesa de Engenharia de Estruturas*, 42:15–18.

Parisi, M. and Piazza, M. (2000). Mechanics of plain and retrofitted traditional timber connections. *Journal of Structural Engineering*, 126(12):1395–1403.

Piazza, M. and Del Senno, M. (2001). Proposals and criteria for the preliminary evaluation, the design and the execution of works on ancient load bearing timber structures. In *Wooden Handwork/Wooden Carpentry: European Restoration Sites*, pages 263–277, Paris, France. Elsevier.

Piazza, M., Tomasi, R., and Modena, R. (2005). *Strutture in legno. Materiale, calcolo e progetto secondo le nuove normative europee*. Ulrico Hoepli, Milan, Italy.

Rinn, F. (1992). Chancen und grenzen bei der untersuchung von konstruktionshölzern mit der bohrwiderstandsmethode. *Bauen mit Holz*, 9:745–748.

Sandoz, J., Benoit, Y., and Demay, L. (2000). Wood testing using acousto-ultrasonic. In *Proceedings of the 6th World Conference on Timber Engineering*, British Columbia, Canada.

Turrini, G. and Piazza, M. (1983). Il recupero dei solai in legno. Esperienze e realizzazioni. *Recuperare,(5)–(7), Milan, Italy*.

UNI 11035-1 (2003). *Structural timber - Visual strength grading for Italian structural timbers: terminology and measurement of features*. Ente Nazionale Italiano di Unificazione.

UNI 11035-2 (2003). *Structural timber - Visual strength grading rules and characteristics values for Italian structural timber population*. Ente Nazionale Italiano di Unificazione.

List of Figures

List of Tables

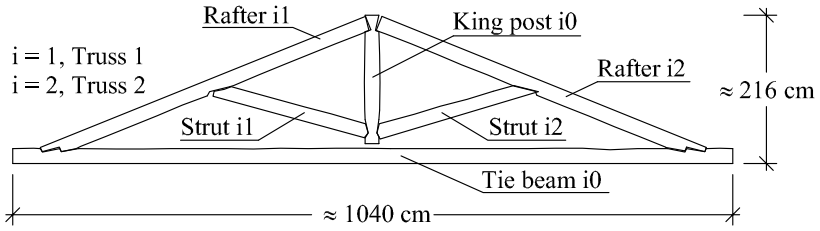

Figure 1: Scheme of the two King-post trusses evaluated with the rule adopted for numbering the timber elements.

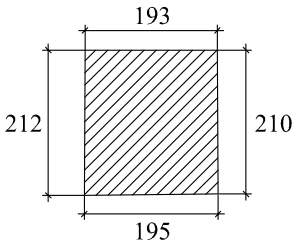

Area = 409.3 cm^2
Principal moment I = 15188 cm^4
Principal moment J = 12837 cm^4

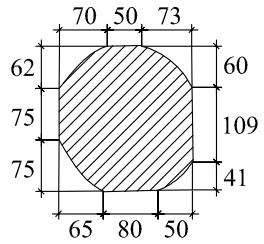

Area = 349.3 cm^2
Principal moment I = 10673 cm^4
Principal moment J = 8898 cm^4

Figure 2: Comparison between the geometric properties of the cross-sections: a) supposing rectangular and b) with detailed measurements (dimensions in millimeters).

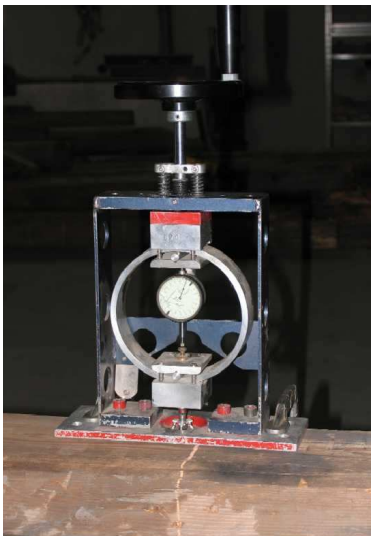

Figure 3: Hardness test device (Turrini and Piazza, 1983).

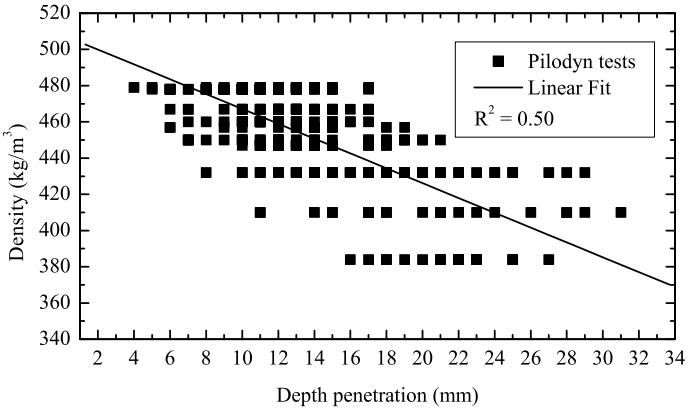

Figure 4: Correlation between depth penetration obtained with Pilodyn® and density

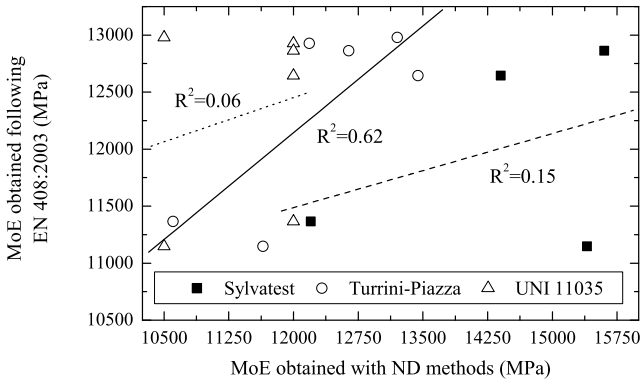

Figure 5: Correlation between MoE values given by non-destructive methods and found through mechanical evaluation according EN408 (2003).

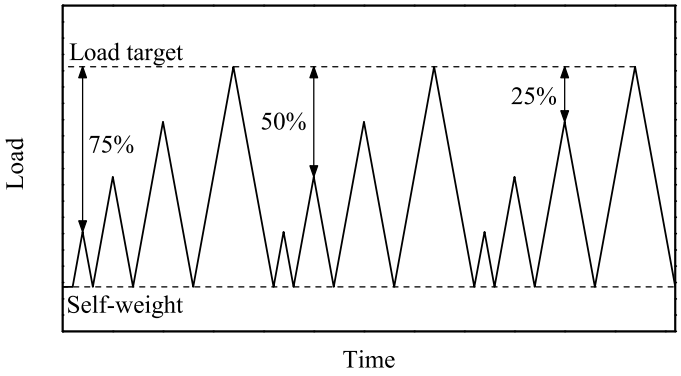

Figure 6: Load procedure applied in the load-carrying tests.

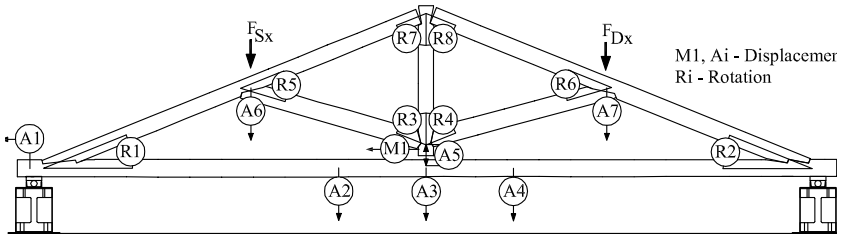

Figure 7: Instrumentation layout.

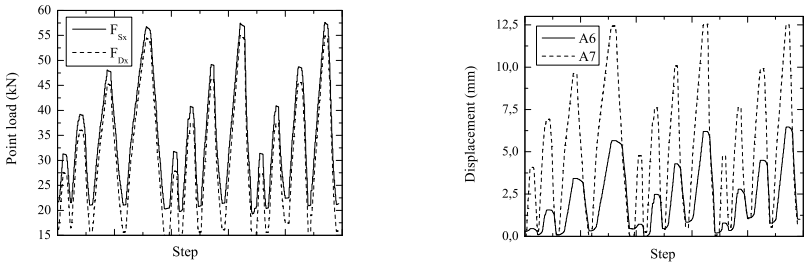

(a) Point loads

(b) Global displacement

Figure 8: Asymmetric behaviour of $Truss$ 1 under symmetric loading condition (S-U-S).

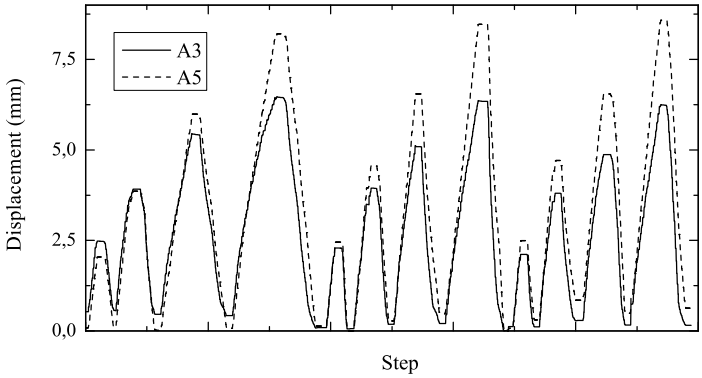

Figure 9: Behaviour of the connection between the king post and the tie beam under symmetric loading conditions.

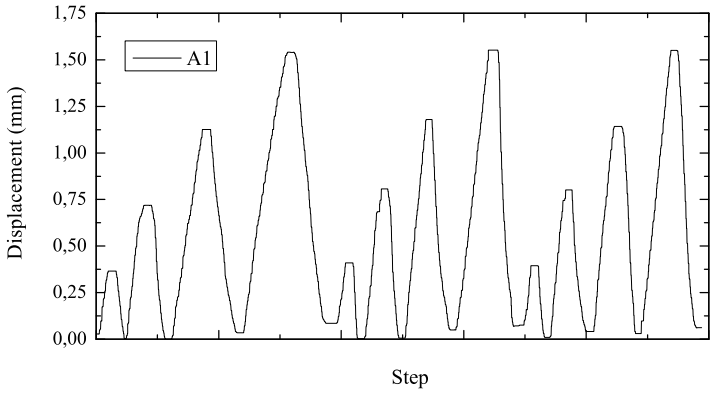

Figure 10: Horizontal displacement recorded in the supports under symmetric loading.

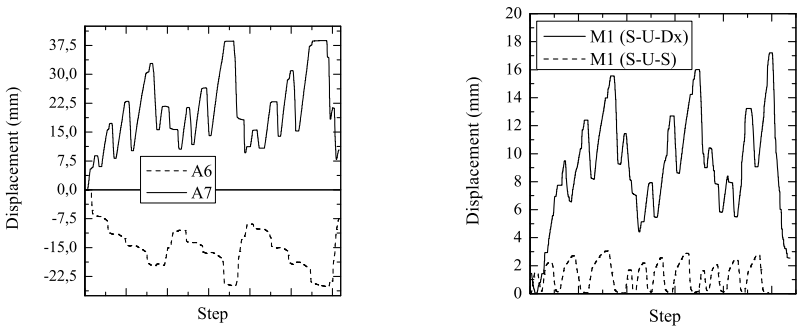

(a) Global displacement

(b) M1 displacement

Figure 11: Asymmetric behaviour emphasised under non-symmetric loading of *Truss* 1 during S-U-Dx test.

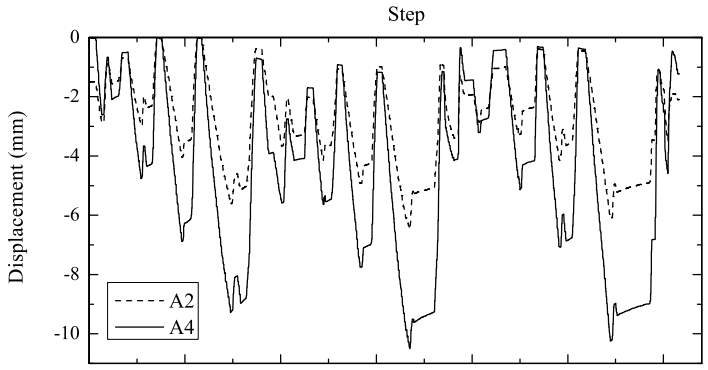

Figure 12: Distortion of the tie beam under non-symmetric loading of $Truss$ 1 during S-U-Sx test.

(a) In the plane truss

(b) In the normal plane of the truss

Figure 13: Bending of the steel rod inserted in the tie connection.

Figure 14: Out-of-plane movement observed in the *Truss* 1 (unstrengthened) under ULS at the end of 1st cycle.

(a) UPN profile preventing the out-of-plane movements in the king post-tie beam connection

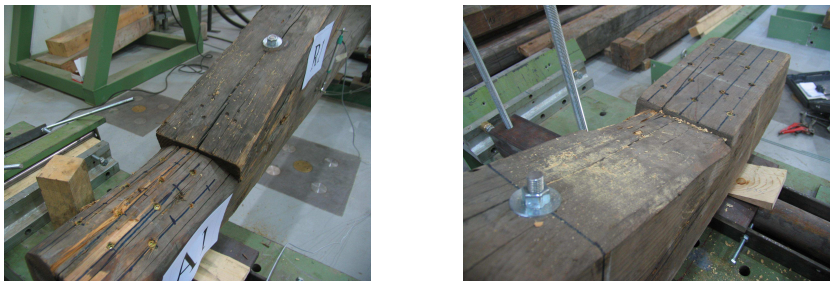

(b) Screws and internal bolt to strength the rafter-tie beam connections

Figure 15: Strengthening of *Truss* 1.

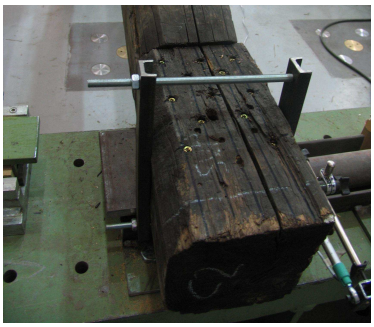

Figure 16: Strengthening of *Truss* 2. Screws and binding strip applied in the step front of the rafter-tie beam connection.

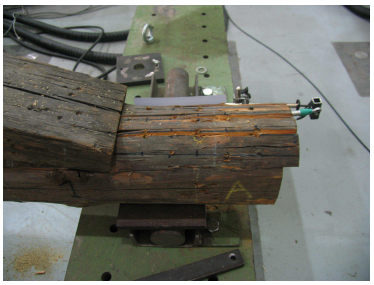

(a) Shear failure in the notch front

(b) Failure of the rear step

(c) Disassemble of king post-struts joint

(d) Bending of the internal bolt

Figure 17: Failure damages of *Truss* 1.

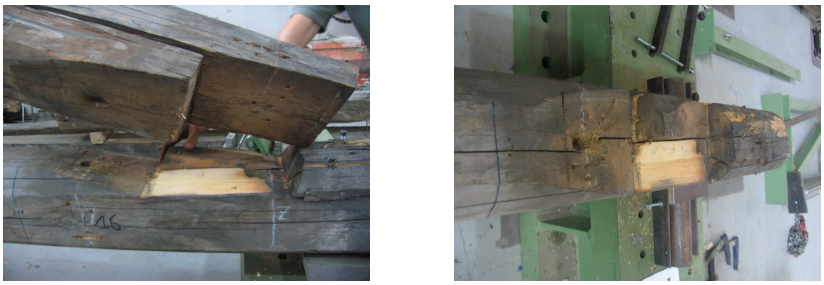

(a) (b)

Figure 18: Shear failure of the tie beam-rafter connection for *Truss* 2.

(a) Failed (right side)

(b) Safe (left side)

Figure 19: Double step connections between the rafters and the tie beam of *Truss* 2.

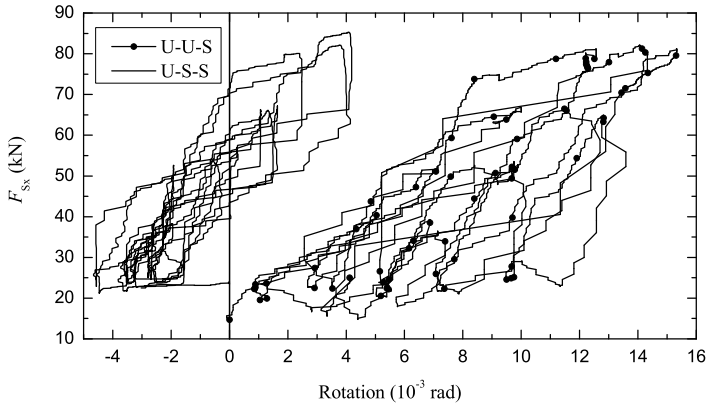

Figure 20: Moment-rotation response of the left rafter-tie beam connection of *Truss* 2 under unstrenghthened and strengthened conditions.

Table 1: Moisture content values (%) measured in each element of both trusses.

Element	*Truss* 1	*Truss* 2
King post	11.7	12.7
Tie beam	12.2	12.4
Strut 1	11.5	12.2
Strut 2	11.3	12.3
Rafter 1	12.5	12.8
Rafter 2	11.9	12.1

Table 2: Density values for each element of the two trusses studied.

Element	Volume (m^3)	Mass (kg)	Moisture (%)	Density (kg/m^3)
King post 10	0.0712	32	11.7	450
Tie beam 10	0.4207	201	12.2	478
Strut 11	0.1009	43	11.5	432
Strut 12	0.0951	39	11.3	410
Rafter 11	0.2014	94	12.5	467
Rafter 12	0.1736	79	11.9	460
King post 20	0.0700	32	12.7	457
Tie beam 20	0.4280	185	12.4	432
Strut 21	0.0730	28	12.2	384
Strut 22	0.1001	45	12.3	450
Rafter 21	0.1922	92	12.8	479
Rafter 22	0.1836	82	12.1	447
		Average	12.1	446
		CoV(%)	6	4

Table 3: Results of the visual strength grading according to UNI 11035 (2003).

Element	Strength Class	$E_{0,\text{mean}}$ (MPa)
King post 10	S1	12000
Tie beam 10	S2	10500
Strut 11	S1	12000
Strut 12	S2	10500
Rafter 11	S2	10500
Rafter 12	S1	12000
King post 20	S1	12000
Tie beam 20	S1	12000
Strut 21	S2	10500
Strut 22	S3	9500
Rafter 21	S1	12000
Rafter 22	S1	12000

Table 4: Elastic modulus estimated by means of the Turrini-Piazza hardness test.

Element *Truss* 1	$E_{0,\text{mean}}$ (MPa)	Element *Truss* 2	$E_{0,\text{mean}}$ (MPa)
King post 10	10991	King post 20	12316
Tie beam 10	13202	Tie beam 20	12183
Strut 11	9572	Strut 21	10312
Strut 12	8447	Strut 22	12156
Rafter 11	11646	Rafter 21	13443
Rafter 12	10605	Rafter 22	12640

Table 5: δ factors calibrated based on the MoE tests results.

Element	Strength Class	δ
Tie beam 10	S2	0,60
Rafter 11	S2	0,58
Rafter 12	S1	0,65
Tie beam 20	S1	0,64
Rafter 21	S1	0,57
Rafter 22	S1	0,61

Table 6: Depth penetration mean values measured with the Pilodyn®.

Element	Number tests	Moisture (%)	Density (kg/m^3)	Depth penetration (mm)	
				Mean	Range
King post 10	20	11.7	450	16.25	7-21
Tie beam 10	104	12.2	478	10.41	5-17
Strut 11	24	11.5	432	19.63	10-29
Strut 12	24	11.3	410	20.42	11-31
Rafter 11	52	12.5	467	12.38	6-17
Rafter 12	48	11.9	460	11.98	7-17
King post 20	20	12.7	457	13.10	6-19
Tie beam 20	104	12.4	432	15.68	8-23
Strut 21	24	12.2	384	21.42	16-27
Strut 22	24	12.3	450	10.75	7-15
Rafter 21	52	12.8	479	11.54	4-17
Rafter 22	52	12.1	447	13.62	10-18

Table 7: Sylvatest® results for the element Rafter 22.

Method	Surface	Length (mm)	Time (μs)	Class	E_b (MPa)	F_b (MPa)
Direct	—	5.1	824	0	15600	30
B-F	Base	1.6	268	0	14800	26
H-L	Base	1.6	269	0	14600	24
B-L	Base	4.0	778	H	—	—
B-F	Left	1.6	265	0	15400	30
H-L	Left	1.6	267	0	15000	26
B-L	Left	4.0	959	H	—	—

Table 8: Sylvatest® results using the direct method.

Element	Moisture (%)	Length (m)	Time (μs)	Class	E_b (MPa)	F_b (MPa)
King post 10	11.7	1.88	329	0	13200	18
Tie beam 10	12.2	10.33	—	—	—	—
Strut 11	11.5	2.23	400	1	12200	12
Strut 12	11.3	2.23	393	1	12800	16
Rafter 11	12.5	5.10	850	0	15400	28
Rafter 12	11.9	4.85	869	1	12200	12
King post 20	12.7	1.87	315	0	14600	24
Tie beam 20	12.4	10.50	—	—	—	—
Strut 21	12.2	2.32	400	0	13600	20
Strut 22	12.3	2.42	459	3	—	—
Rafter 21	12.8	5.10	864	0	14400	28
Rafter 22	12.1	5.11	824	0	15600	30

Table 9: MoE obtained by means of four-point bending tests.

Element (*Truss* 1)	$E_{\mathrm{m,l}}$ (MPa)	Element (*Truss* 2)	$E_{\mathrm{m,l}}$ (MPa)
Tie beam 10	12980	Tie beam 20	12929
Rafter 11	11149	Rafter 21	12646
Rafter 12	11367	Rafter 22	12863

Table 10: Load-carrying tests performed.

Test	*Truss* 1		*Truss* 2	
	F_{Sx} (kN)	F_{Dx} (kN)	F_{Sx} (kN)	F_{Dx} (kN)
S-U-S	57.6	55.0	40.5	46.2
S-U-Dx	25.7	47.9	34.2	53.7
S-U-Sx	58.4	30.9	61.9	34.9
U-U-S	65.8	68.7	82.2	84.6
U-U-Dx	n.p.	n.p.	44.4	82.9
U-U-Sx	n.p.	n.p.	82.8	44.9
S-S-S	65.8	68.7	61.0	63.7
S-S-Dx	22.1	44.3	31.7	59.1
S-S-Sx	45.4	27.4	61.9	30.9
U-S-S	74.5	69.0	85.8	85.7
U-S-Dx	n.p.	n.p.	41.8	83.6
U-S-Sx	n.p.	n.p.	84.2	44.2
Failure	54.6	55.2	108.1	107.5

n.p. - test not performed

Table 11: Maximum displacement recorded by the instrumentation setup during the load-carrying tests on *Truss 2*.

Order	Test	F_{Sx} (kN)	F_{Dx} (kN)	M1 (mm)	A1 (mm)	A2 (mm)	A3 (mm)	A4 (mm)	A5 (mm)	A6 (mm)	A7 (mm)
1st	S-U-S	39.8	43.2	3.4	1.9	7.0	6.6	6.6	6.8	12.8	13.1
2nd	S-U-Dx	30.2	53.7	12.1	2.4	5.4	7.2	9.6	8.0	10.3	25.7
3rd	S-U-Sx	60.7	24.8	10.7	1.2	7.7	6.4	4.9	6.2	30.5	18.1
4th	U-U-S	82.2	83.3	8.1	3.3	13.3	13.1	12.1	13.1	21.2	20.0
5th	U-U-Dx	39.3	81.8	15.9	3.0	6.4	8.8	11.7	9.2	18.3	38.9
6th	U-U-Sx	82.0	43.5	12.7	2.1	11.9	9.5	7.0	14.6	46.8	24.3
7th	S-S-S	58.9	63.4	3.5	2.6	10.3	11.0	11.1	8.9	11.0	20.5
8th	S-S-Dx	28.8	59.1	9.4	2.1	4.4	6.1	8.4	6.1	15.4	26.8
9th	S-S-Sx	61.9	28.0	18.5	1.2	9.5	6.6	4.7	7.2	34.4	22.0
10th	U-S-S	84.9	85.6	2.3	3.3	10.9	10.4	9.9	11.0	19.0	19.2
11th	U-S-Dx	39.8	81.5	10.4	3.2	6.6	9.2	11.7	9.4	18.9	33.0
12th	U-S-Sx	81.3	42.7	7.9	1.8	13.6	10.3	7.3	14.3	44.1	23.8